International Journal of Heat and Technology
Vol. 43, No. 1, February, 2025, pp. 125-138
Journal homepage: http://iieta.org/journals/ijht

Utilizing Solar and Geothermal Energies for Sustainable Room Cooling: A Case Study

Muntadher H. Abed[1,2*], Mohammed I. Mohsin[2], Hasaanein M. Hussein[2]

[1] Institute of Technology-Baghdad, Middle Technical University, Baghdad 29036, Iraq
[2] Mechanical Engineering Department University of Technology, Baghdad 10066, Iraq

Corresponding Author Email: engmuntadher.alsafi1987@gmail.com

https://doi.org/10.18280/ijht.430114

Received: 11 November 2024
Revised: 30 January 2025
Accepted: 14 February 2025
Available online: 28 February 2025

Keywords:
ground source heat pump, renewable energy, zero building, cooling coefficient of performance (COP)

ABSTRACT

Most cooling applications rely on fossil fuels; however, this study developed a hybrid cooling system that utilizes solar and geothermal energy to cool a room. The solar energy system provided an electrical power of 4400 watts, while the geothermal energy harnessed the earth's subsurface coolness to chill the refrigerant. The system primarily consisted of the following components: an air-conditioned space, a modified split-type air-conditioning unit, a solar power system, a cooling water circulation system, and a measurement and control system. The study was conducted in the Aoun area of Karbala City, Iraq, which experiences a hot climate. The testing periods covered daytime and nighttime conditions. The research focused on assessing the effect of varying the cold water flow rates supplied to a modified split unit system. Four flow rates were considered: 2.5, 3, 7.5, and 18 liters per minute. The findings indicate that the optimal cooling performance was achieved at a flow rate of 18 liters per minute, where the system attained a cooling coefficient of performance (COP) of 5.26. At this flow rate, the coolant temperature remained within an effective range for space cooling. Furthermore, the system demonstrated a sustainable and environmentally friendly solution, as it operated entirely on renewable energy, powering both the cooling system and all other devices within the space while generating a 15% surplus of the supplied energy. Notably, WFRL4 exhibited a COP that was over seven times higher than that of WFRL1, underscoring its superior efficiency. At the highest flow rate, the system enabled the building to function as a Zero Energy Building (ZEB), further reinforcing its sustainability credentials. Additionally, the cooling efficiency of the system significantly surpassed that of conventional air-cooled systems, with a 54% improvement in COP. Overall, this study introduces a highly efficient and eco-friendly cooling model, offering a sustainable alternative that eliminates harmful emissions and enhances energy efficiency, making it a viable solution for future applications in energy-conscious environments.

1. INTRODUCTION

Environmental pollution has escalated to its peak in recent years, and air pollution stands out as one of the major concerns. The major cause of air pollution is fossil fuel-based HVAC systems. Firstly, such systems are energy guzzlers, potentially consuming almost 40% of the energy produced [1]. Secondly, they are major emitters of harmful gases; they contribute about 35% of these emissions. One of the main pollutants is carbon monoxide, which is responsible for global warming and the depletion of the ozone layer [2]. Recent studies have focused on reducing these percentages by developing systems that work using renewable sources of energy: solar energy and geothermal energy for conditioning space. The basic properties on which researchers base their work are the respective properties of conditioning processes.

Indeed, some researchers have directed their interests to employ geothermal energy through heat pumps for heating and cooling using the earth's subsurface characteristics, as shown in Conguedo et al. [3]. Some other researchers have exploited solar and geothermal properties in producing hybrid systems for space conditioning; Palomba et al. is an example [4].

A ground source heat pump (GSHP) is a modern HVAC system that uses geothermal energy for heating and cooling applications. The system works by extracting heat from the ground and transferring it to a designated space for heating, while in cooling mode, it reverses the process by absorbing heat from the building and dissipating it into the ground. There are two main types of GSHPs: horizontal systems, which are installed at shallow depths of 1 to 1.5 meters, and vertical systems, which operate at depths of up to 200 meters and are ideal for locations where land availability is limited but greater thermal stability is required. Geothermal heat pumps have been a focus of varied depth with researchers. For example, a study by Hussen and Hisham [5] using a heat pump installed at 7.25 meters to cool space in Baghdad, Iraq, attained a cooling coefficient of performance (COP) of 2.574. As observed, geothermal heat pumps generally outperform air-source heat pumps. In the study for comparison researched by Santos et al. [6], where his geothermal system used R410a as

the refrigerant, results showed a superior COP of 5.9 in hot climates in Brazil. Compared to an air-source heat pump that achieved a COP of 3.7, this signifies a 59% performance improvement toward the geothermal system. Ghafoor and Khdir [7] investigated an alternative method of cooling which involved an underground pipe as a heat exchanger 31 m long with a diameter of 10 cm. It was buried at a depth of 3 m beneath the soil in Erbil, Iraq. Air was forced through the pipe at a flow rate of 195 cubic meters per hour. The results indicated that room temperature was reduced from 35°C to 20-23°C, and the COP approached 5.13. Another study developed a multi-layer composite pipe-based heat exchanger system by Omran et al. [8]. Several water flow rates for cooling space were tested in this study, and it was found that the COP increased with higher flow rates. For instance, at a flow rate of 0.5 liters per minute, the COP was 2.28; at 3 liters per minute, it rose significantly to 7.37. Others have turned to improving the performance of geothermal heat pumps. The double U-shaped plastic heat exchange tubes were installed at a deep borehole of 56 m for Yasukawa et al. [9]. In this study, the climate is Thailand, the COP of cooling equals 3, and the energy-saving value reaches 0.6 kW. An upcoming study in South Korea by Hwang et al. [10] applied a heat exchanger with 24 deep boreholes functioning as a geothermal heat pump to air-condition a school during the summer. The paper compares the system's performance to an air-source heat pump. According to their report, the COP of the geothermal heat pump is 8.3 compared to that of the air-source heat pump, which is 3. Naili et al. [11] A 100-metre long horizontal pipe at 1-metre depth acted as a water-to-water heat exchanger to cool the refrigerant R410a in a heat pump. This was a device mounted in a room of 12 square meters in Tunisia. The results gave a value of the COP of 2.88, which is good for building-cooling applications in Tunisia. Omer [12] concluded that energy consumption issues and energy conservation directions could be effectively addressed by geothermal heat pump technology. The study showed that the yearly coefficient of performance was 3.16, while for cooling, it reached 3.43. This technology is environmentally friendly and economically viable in terms of energy-saving.

Most previous work has focused on using geothermal energy for cooling, with scant attention paid by researchers to methods of saving energy in the systems operation and performance improvement. The depths applied in Iraq's climate were relatively low. The major aim of our experimental work is to install a cooling system that is operational and entirely eco-friendly and operates on renewable energy sources by integrating it with a GHP. The whole system is solar-powered. The other major aim is to consume less energy and generate extra energy, which can power other devices in the room or elsewhere.

2. EXPERIMENTAL SETUP AND METHODOLOGY

The principle of operation for the heat pump in cooling mode is to utilize the low temperatures found underground during the summer. This is achieved by circulating a fluid to a certain depth, directly cooling the space, or chilling a refrigerant fluid [13]. There are two types of geothermal heat pumps: horizontal systems, which are installed at shallow depths of up to 1.5 meters, and vertical systems, which are installed at much greater depths, sometimes reaching up to 200 meters [14]. In this study, an experimental model was examined, as shown in Figures 1 and 2, consisting of the following components

- The air-conditioned space (room)
- Modified split unit type air-conditioning unit.
- Solar power system
- Cooling water circulation system
- Measurement and control system

Case study

The agricultural office room, with a total area of 12.75 m², is located in the Aoun region, north of Karbala, at geographical coordinates 32.6° latitude and 44.02° longitude. Designed as a functional workspace for agricultural tasks, the room has essential office furniture, including a laptop computer, two office chairs, a water cooler, a coffee maker, a printer, and a desk. The total energy consumption of the office is 1750 watts, including a water pump used for crop irrigation. Figure 3 illustrates the office room that was analysed in this study.

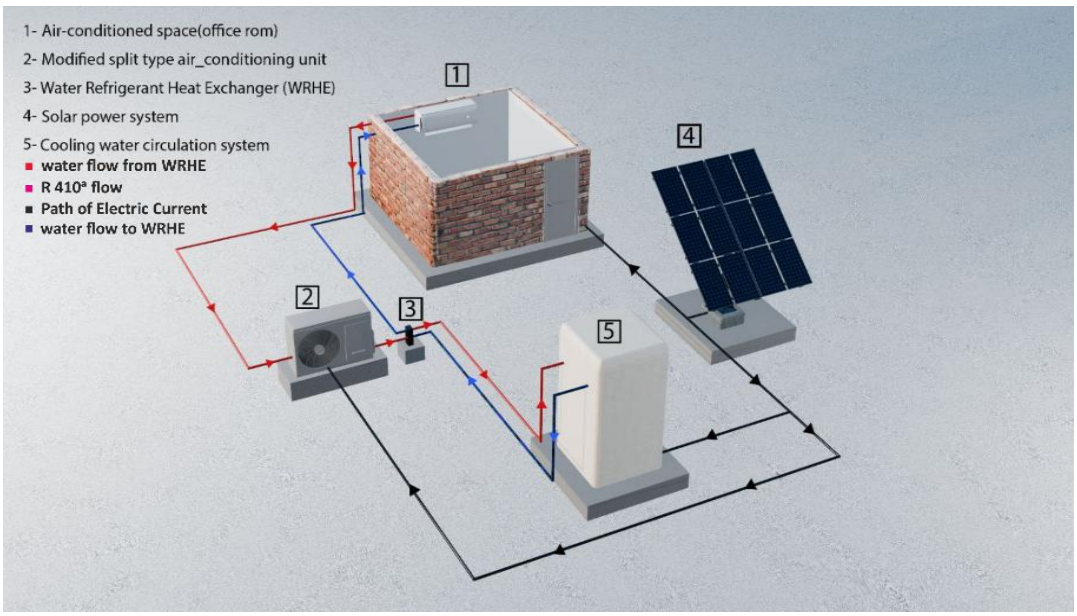

Figure 1. Description of the system

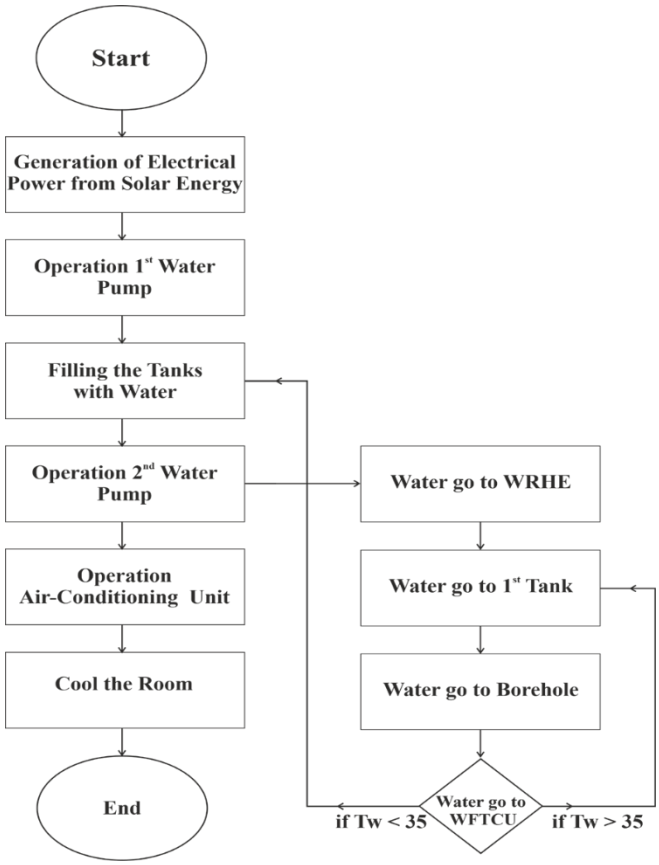

Figure 2. Algorithm representing the operational steps of the system

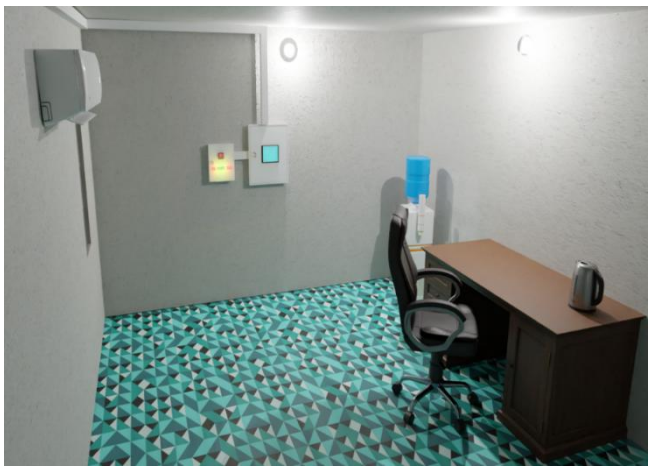

Figure 3. Office room

System Components

i. Modified split type air-conditioning unit

The modified split unit air conditioner, a General Electric model GESFBH180OUAAR, has a cooling capacity of 18,000 Btu/hour and incorporates traditional components such as a compressor, condenser, expansion valve, and evaporator. It utilizes R410a refrigerant, has high efficiency, and is classified as an environmentally friendly refrigerant, as it does not deplete the ozone layer. It complies with international environmental laws and regulations. Moreover, it possesses the capability to withstand high pressures [15]. Key modifications include operating the system on solar energy and replacing the air-cooled condenser with a heat exchanger that uses groundwater for cooling.

ii. Water-Refrigerant Heat Exchanger (WRHE)

A stainless-steel plate heat exchanger was used for cooling devices like split units and floor cooling systems. It features a parallel flow design and operates efficiently across various temperatures and pressures. The unit has four openings for refrigerant and water inlets and outlets (Figure 4), utilizing R410a as the primary fluid and cooled water as the secondary fluid. It has a cooling capacity of 18,000 - 24,000 (BTU/h).

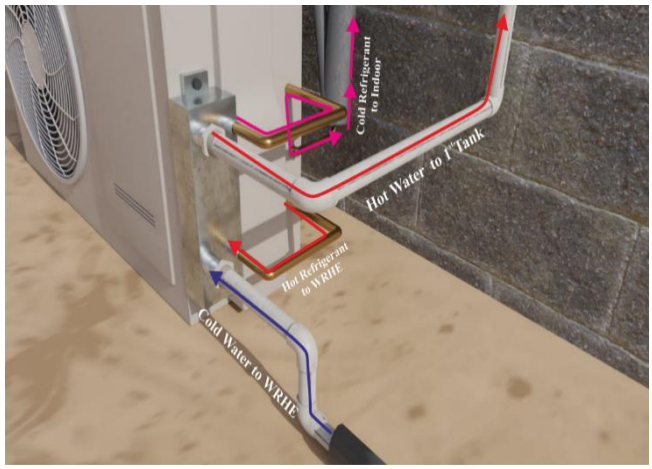

Figure 4. Flow of cold water and refrigerant within the heat exchanger

iii. Solar power system

The solar power system is designed for a room, and the air conditioner generates approximately 4,000 watts using 12 mono-crystalline solar panels, as shown in Figure 5, which are optimized for high temperatures. It includes Eastman TTC lead-acid batteries for nighttime energy storage and an inverter for voltage conversion. The system is interconnected to power the cooling system and other devices in the agricultural office, ensuring efficient energy use.

Figure 5. Solar panels prepared for electrical energy generation

iv. Cooling water circulation system (CWCS)

The CWCS in conditioner is designed to leverage groundwater's naturally lower temperatures for cooling without using groundwater directly due to its high salinity and potential for corrosion and mineral deposits. Instead, clean water from a reservoir is circulated through a borehole to absorb the coolness from the ground. The borehole, drilled to a depth of 24 meters and lined with PVC pipes, allows

groundwater to cool the clean water while preventing soil and sediment from entering the pipes. After drilling, external water flushing removes clay and sediment to maintain efficient thermal exchange. A galvanized iron Water-Water Heat Exchanger (WWHE), shaped in a U-form and extending 21 meters into the borehole, transfers heat between the warm water from the system and the cold underground water. Insulation on the upper 7 meters of the pipe prevents reverse heat exchange. The system incorporates three water tanks and two pumps. The primary tank supplies water to the WWHE, the second tank stores cooled water, and the third tank distributes this to the air conditioning system. The entire network, including insulated PVC pipes and high-quality needle valves, ensures consistent water flow and minimal heat loss, enhancing system efficiency. This design effectively utilizes groundwater's cooling properties while protecting the system from corrosion and ensuring long-term performance in air conditioning applications. Figure 6 illustrates the schematic of the water colling circulation system.

Experiments Description

i. Basic experiments

All experiments utilized a consistent water flow rate of 2 liters per minute from the main tank into the borehole. The flow rate for cooling the refrigerant in the heat exchanger was tested at three levels: low (2-3 liters per minute), medium (7.5 liters per minute), and high (18 liters per minute). Table 1 presents the various water flow rate levels.

ii. Operating conditions

The system operates under steady flow conditions, adhering to the Continuity Equation across all components. It is a closed and thermally insulated system, ensuring the water temperature remains stable despite external conditions. The flow is uniform, with no head losses affecting the rate, and it maintains thermal balance, where heat gained equals heat lost. Operations are scheduled for daytime from 11:00 a.m. to 3:00 p.m. (Test Period 1) and evening from 8:00 p.m. to 10:00 p.m. (Test Period 2).

iii. Measurement and control devices

A Programmable Logic Controller (PLC) system was implemented to monitor and display temperature and current readings. Key components included a Delta DVP 12SS2 CPU for data processing, DELTA input modules for signal reception, and a DELTA DOP-107V Human-Machine Interface for data display. Temperature measurements were taken using type K thermocouples and Resistance Temperature Detectors (RTD) at various depths. A Water Flow – Temperature Control Unit (WFTCU) utilises solenoid valves and temperature controllers to regulate water temperature for cooling, ensuring efficient operation.

Table 1. Various water flow rate levels

Water Flow Rate Level (WFRL)	Value(l/min)
WFRL 1	2
WFRL 2	3
WFRL 3	7.5
WFRL 4	18

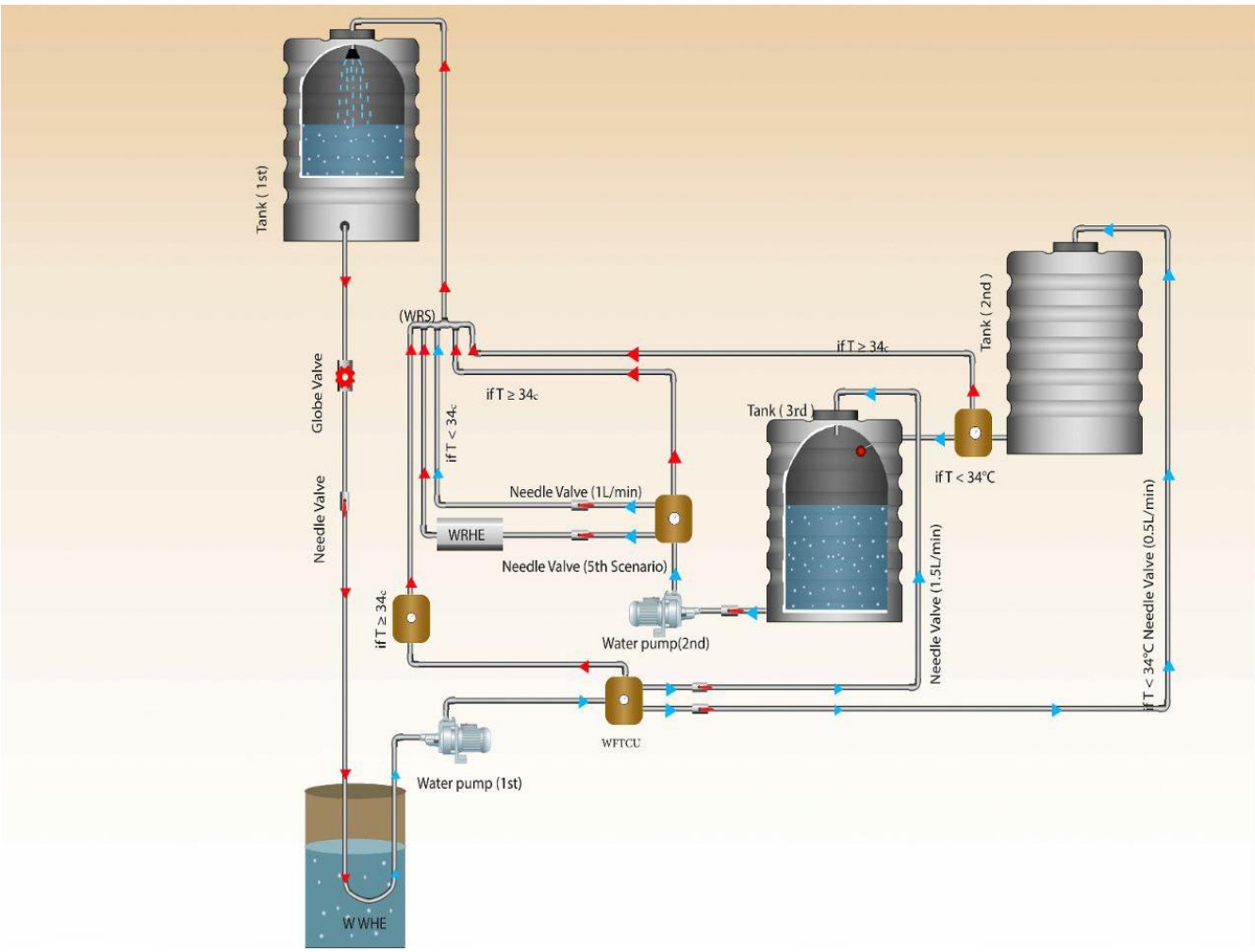

Figure 6. Schematic of CWCS

3. COMPLEMENTARY CALCULATIONS

3.1 Cooling load calculations for office room

A. Cooling loads due to external heat gain

Heat gain through walls and ceilings arises from two main factors: the steady heat transfer due to the temperature difference between internal and external air and the unsteady heat gain from varying solar radiation on the walls' surfaces. These components are analyzed using the Cooling Load Temperature Difference (CLTD) method, which helps calculate the sensible heat gain from these influences [16].

$$Q = A\times U \times CLTD \quad (1)$$

Cooling load due to heat gain through doors and glass:

For doors [16]:

$$Q = Ud\times Ad \times \Delta Tf \quad (2)$$

For glass [16]:

The cooling load from heat gain through glass has two main components. The first component is the conductive heat gain due to the temperature difference between outdoor and indoor air. This conductive heat gain is analyzed similarly to heat gain through walls and ceilings, utilizing the CLTD method.

$$Qg/\ cond=Ug\times Ag\times CLTDc \quad (3)$$

The cooling load from solar heat gain through glass is determined by multiplying the maximum solar heat gain (SHGmax) by a specific cooling load factor [16].

$$Qg/\ sol=Ag\times SC\times SHG\times CLF \quad (4)$$

Ventilation Load: - The sensible and latent heat from the ventilation air can be calculated using the following equations [17].

$$Qvent/\ S=1.23\times Vvent\times(To-Ti) \quad (5)$$

$$Qvent/\ L=3010\times Vvent\times(Wo-Wi) \quad (6)$$

Heat Gain Due to Infiltration: - The sensible and latent heat associated with the infiltrated air can be calculated using the following equations [17]:

$$Qinf/\ S=1.23\times Vinf\times(To-Ti) \quad (7)$$

$$Qinf/\ L=3010\times Vinf\times(Wo-Wi) \quad (8)$$

B. Cooling loads due to internal heat gain

The sensible and latent heat emitted by the occupants (occupant load). The sensible heat emitted by occupants of the space is calculated from the following equation [18]:

$$Qp/\ s=No/p\times qS/P\times CLF \quad (9)$$

The latent heat emitted by occupants of the space is calculated from the following equation [18]:

$$Qp/\ L=No/p\times qL/P\times CLF \quad (10)$$

The load of devices and machinery in Table 2 presents the types of devices used and the heat generated by each device.

Table 2. Heat generated by various electronic devices [19]

Device	Q (watt)
Computer Laptop	60
Water cooler	150
coffee maker	300
Printer	30
Q total	540

Lighting loads are calculated using the following equation [18]:

$$QL=NL\times WL\times Fb \quad (11)$$

The cooling load required for the room was calculated to be approximately 1.5 (BTU/H).

3.2 Effectiveness of the heat exchanger

A heat exchanger's (WRHE) effectiveness measures heat transfer efficiency, calculated as the actual to theoretical heat exchange ratio, influenced by design and fluid flow configuration [19, 20].

$$\epsilon exp=((Thin-Tcout))/((Thin-Tcin) \quad (12)$$

3.3 Performance of air-conditioning unit

Input Power:

$$P=I\times V \quad (13)$$

Coefficient of Performance (COP):

$$COPex=Qrej/P \quad (14)$$

3.4 The energy efficiency ratio (EER)

EER signifies a cooling system's energy utilization efficiency.

It is determined by dividing the system's cooling capacity by the electrical energy consumed by the cooling system.

It is calculated by [21]:

$$EER=3.41\times COPex \quad (15)$$

4. DISCUSSION OF RESULTS

This study evaluated a hybrid cooling system's thermal performance and energy efficiency using water as a coolant instead of air, powered by renewable solar energy. The analysis examined how variations in flow rate impacted thermal changes within the water circulation system, including the borehole, the water-to-water heat exchanger (WWHE), and the pumping system. The cooling performance and energy savings were assessed under four water flow rate levels.

Figure 7 shows the variation in inlet water temperature at the borehole of the WWHE over time, supplied by Tank 1. In Test Period 1, at WFRL1, the inlet temperature initially rises to around 45°C within the first hour, then drops to approximately 30°C before increasing again towards the period's end. A similar but lower peak trend is observed at WFRL2. This suggests that the main tank temperature is high due to the elevated water temperature returning from the

secondary heat exchanger. At WFRL3, temperatures fluctuate between 30°C and 35°C, with a final rise toward the end, while WFRL4 shows a significantly lower temperature, reaching around 20°C. This reduction indicates stable system operation. In Test Period 2, all temperatures were consistently high, reflecting the increased tank temperature due to the elevated temperature of returning water.

Figure 8 illustrates the WWHE's role in cooling via borehole water. In Test Period 1, the exchanger significantly reduced inlet temperatures across all flow rates, with a pronounced effect at WFRL4, where temperatures dropped to around 10°C, remaining below 30°C across all flow rates. In Test Period 2, however, outlet temperatures rose above 30°C, peaking at 35°C, due to thermal accumulation in the borehole from hot water inflow from Tank 1. This reduced the heat exchange efficiency, as inlet and outlet temperatures became nearly identical. The compressor in the refrigeration cycle pressurizes the refrigerant, raising its temperature, but it must stay within safe temperature limits to prevent failure. Effective compressor operation enhances system cooling.

Figure 9 shows fluctuating refrigerant temperatures at the first three flow rates, reaching up to 70°C, while WFRL4 maintained lower, more stable temperatures below 60°C in Test Period 1. In Test Period 2, refrigerant temperatures increased across all flow rates, but WFRL4 remained the most stable, resulting in decreased compressor efficiency. The temperature of R410a exiting the heat exchanger toward the evaporator is optimal when it approaches 10°C [22].

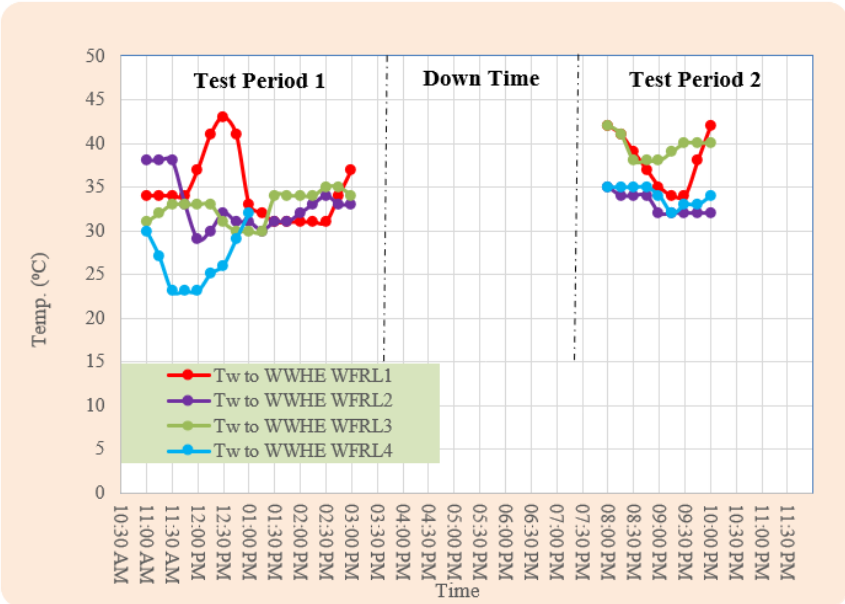

Figure 7. Variation of inlet water temperature with time for WWHE

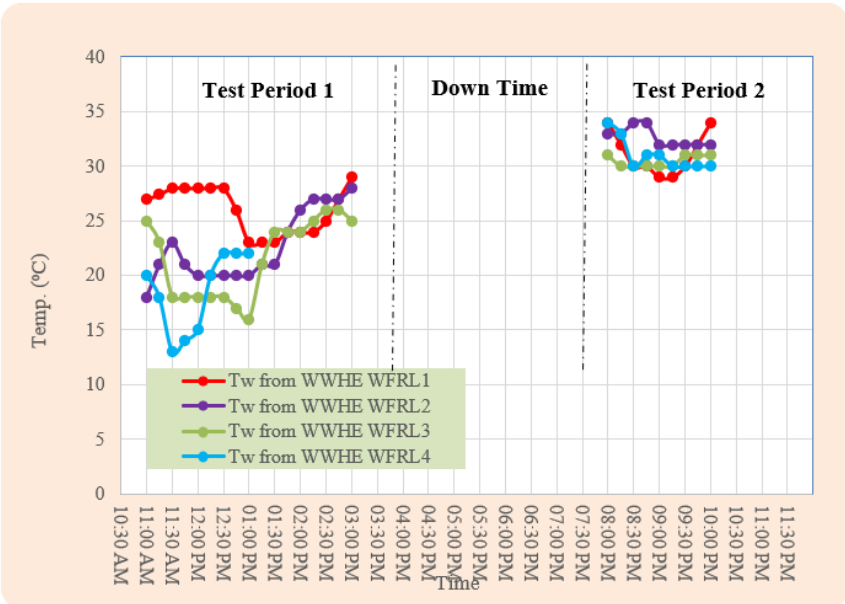

Figure 8. Variation of outlet water temperature with time for WWHE

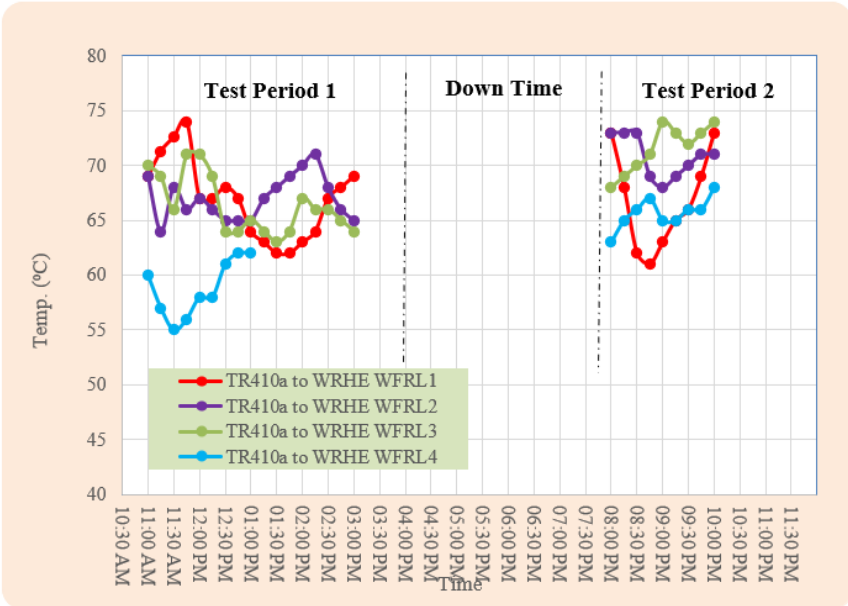

Figure 9. Variation of R410ª temperature with time inlet to WRHE

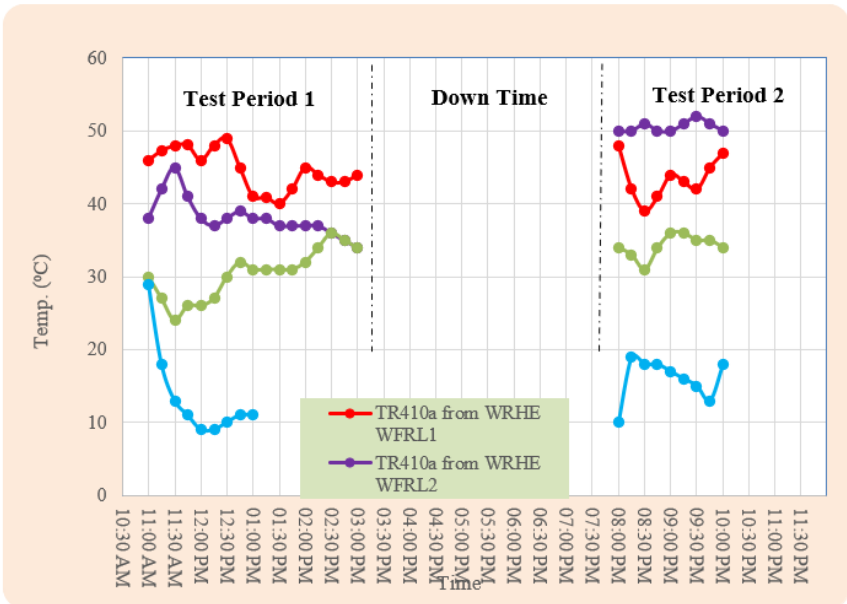

Figure 10. Variation R410ª temperature with time at WRHE outlet

Figure 10 illustrates the refrigerant temperature at various water flow rates. During Test Period 1, the water temperature is high across various flow rates, except for the WERL4, where the temperature remains close to 10°C throughout the operation. This indicates that the cooling rate of the refrigerant increases with higher water flow rates, as a higher flow rate provides a greater heat exchange area, leading to a relatively faster temperature reduction. In Test Period 2, temperatures are higher than in Test Period 1, caused by the increased temperature of the water entering the heat exchanger, as illustrated in Figure 11. Figure 12 also displays the temperature of the water supplied to the WRHE for refrigerant cooling. In Test Period 1, the water temperature was lowest at the WFRL3; however, it was insufficient for cooling the system effectively, as the third flow rate did not provide adequate cooling for the refrigerant. On the other hand, all temperatures remained below 35°C during this period. This temperature threshold was set to shut off flow in the WFTCU during experimental tests, as higher temperatures were not beneficial for cooling. In Test Period 2, there is a noticeable increase in the temperature of the water supplied to the WRHE. At the WFRL1, the temperature exceeded the critical level throughout the operation, proving insufficient for refrigerant cooling, negatively impacting the system's cooling performance. However, at the WFRL4, despite the higher temperature, the high flow rate largely compensated for the temperature rise, resulting in a slight reduction in cooling efficiency.

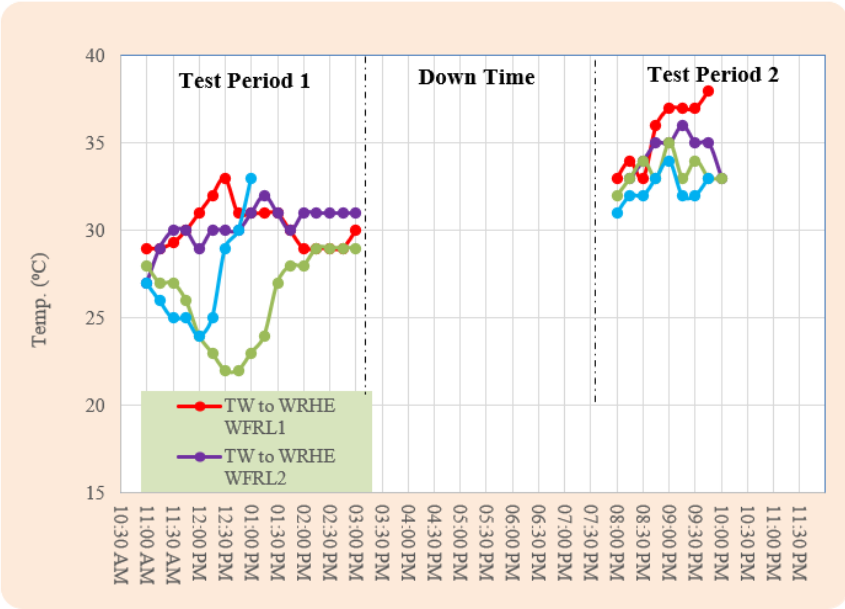

Figure 11. Variation of chilled water supply temperature with time supplied

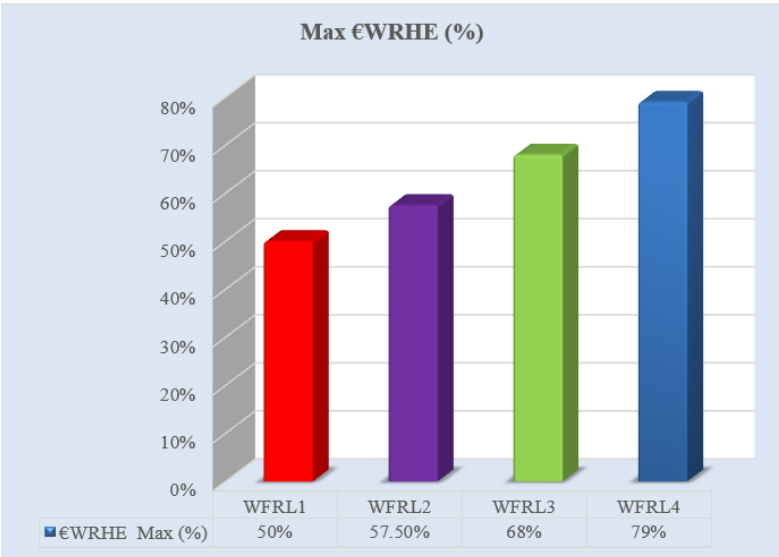

Figure 12. WRHE effectiveness at different water flow rate levels

Figure 13 shows that the WRHE's highest effectiveness in cooling the refrigerant with pre-cooled groundwater was achieved at the WFRL4, reaching 79%. The effectiveness of the heat exchanger increases with higher cold water flow rates. Since the primary goal of this study is to provide a comfortable agricultural office environment, Figure 14 shows that the WFRL4 achieved a comfortable space temperature during Test Period 1, compared to the higher temperatures at other flow rates. The temperature remained below 25°C, close to the optimal comfort level [23]. In Test Period 2, the room temperature was higher, confirming that the cooling efficiency in Test Period 1 was superior due to less thermal accumulation within the borehole. However, the temperature remained relatively good at the WFRL4, close to 25°C. Regarding relative humidity, Figure 15 shows that the WFRL4 maintained a stable level, close to the optimal relative humidity [24], and higher than the other flow rates. In Test Period 1, the relative humidity was around 40%, while in Test Period 2, it was close to 45%, remaining consistently stable. This study also emphasizes selecting the optimal system design for cooling performance, energy consumption, and resource utilization to achieve an eco-friendly solution that provides high cooling efficiency. Figure 16 confirms a direct relationship between the cooling performance coefficient (COP) and the cold water flow rate into the WRHE. The system's optimal performance was achieved at the WFRL4, with a COP of 5.26, exceeding the COP of the WFRL1 (0.66) by more than seven times. The COP at the WFRL1 was very low, rendering the system ineffective for cooling. Figure 17 shows the EER values for the system at different water flow rates, with the highest efficiency in electrical energy use for cooling observed at the WFRL4, where the EER reached 17.96.

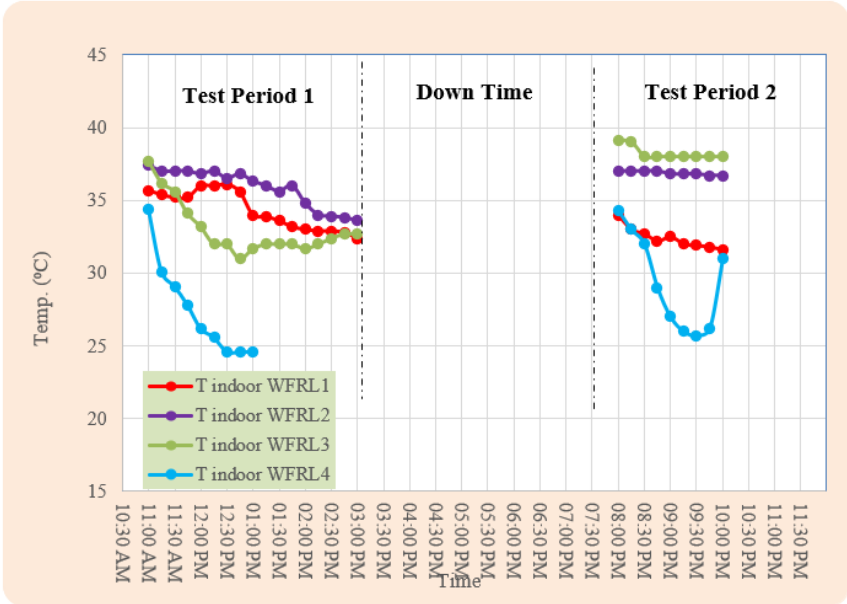

Figure 13. Indoor temperature changes with time

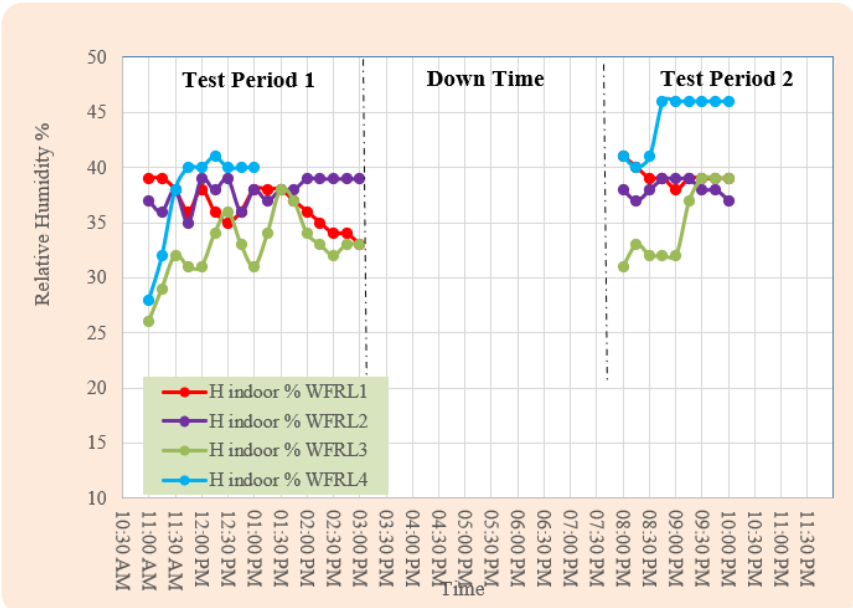

Figure 14. Indoor relative humidity changes with time

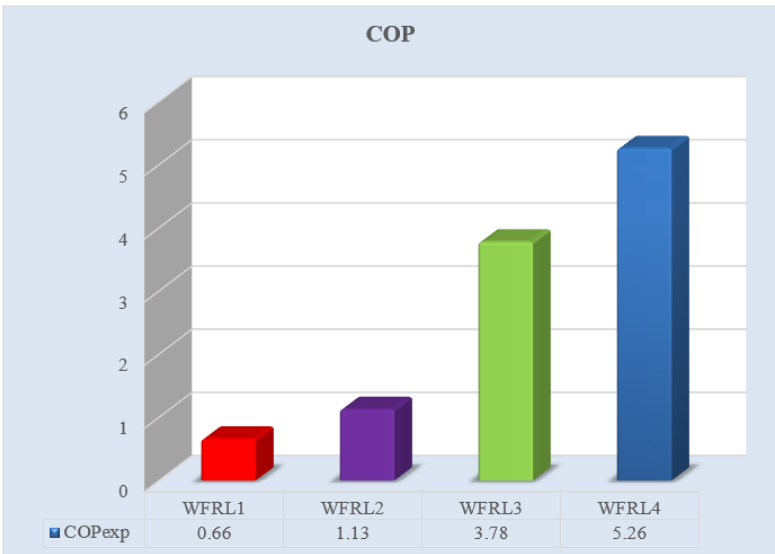

Figure 15. COP at different water flow rates

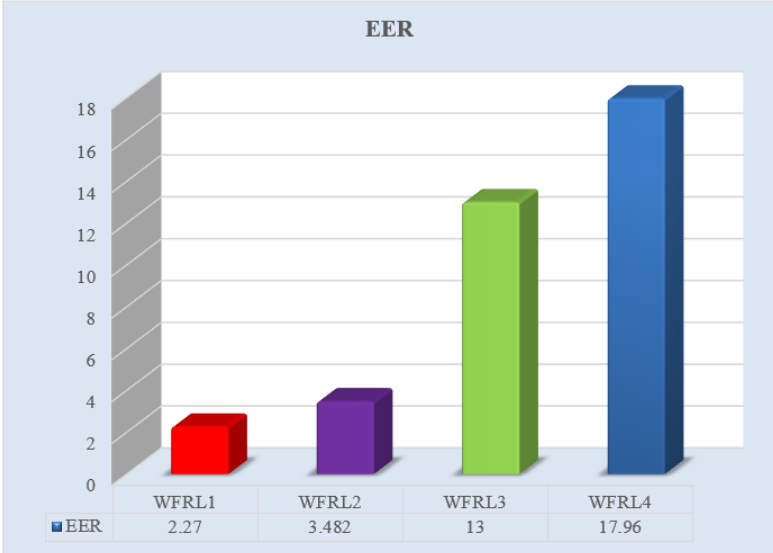

Figure 16. EER of the system at different water flow rates

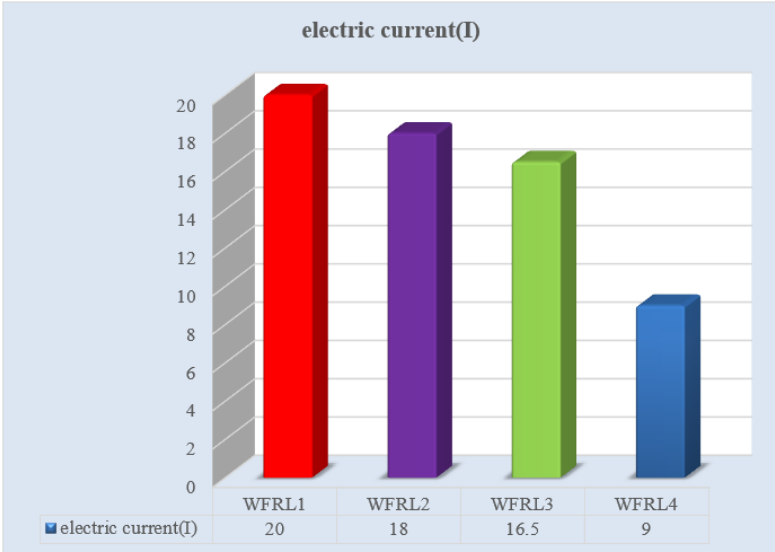

Figure 17. Electrical current of the system at different water flow rates

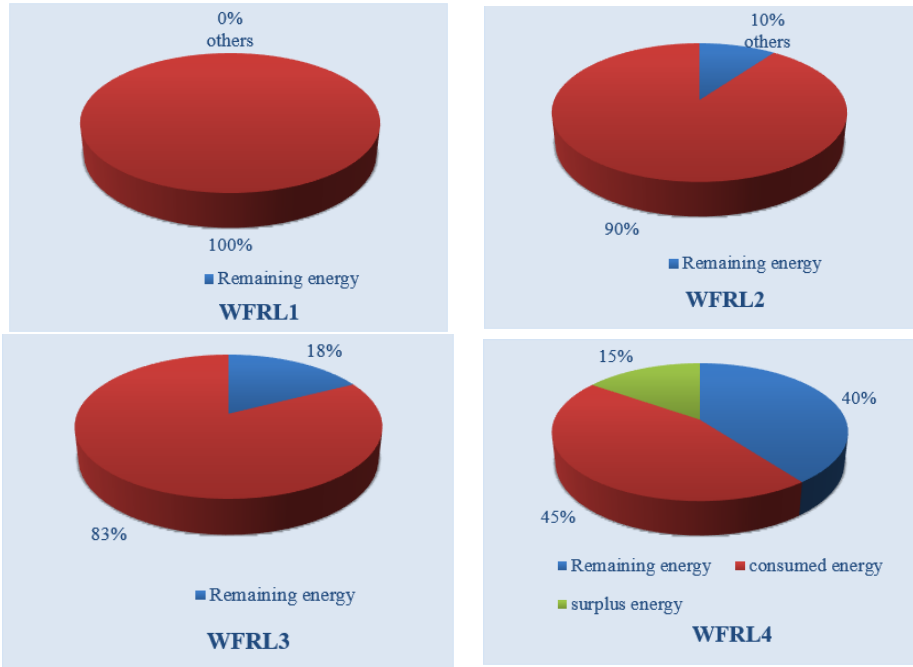

Figure 18. Energy consumption for system operation, other devices, and surplus energy at different water flow rates

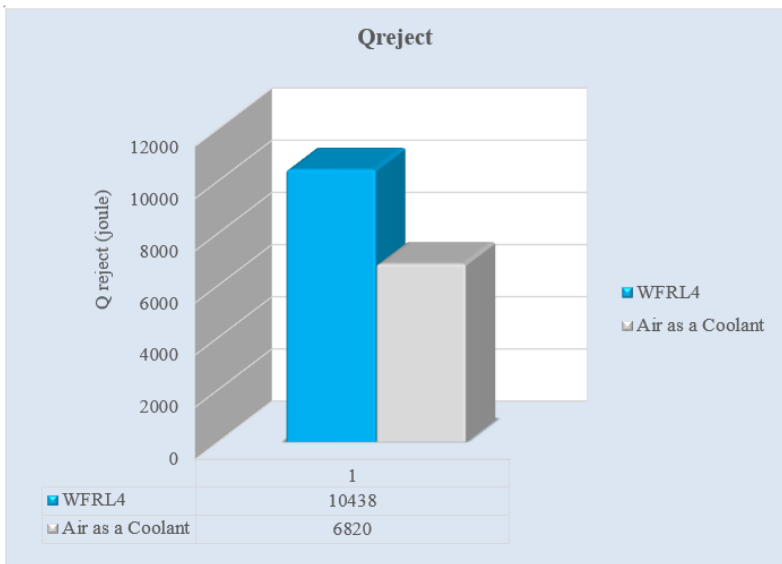

Figure 19. Heat rejection at the WFRL4 compared to using air as a refrigerant cooler

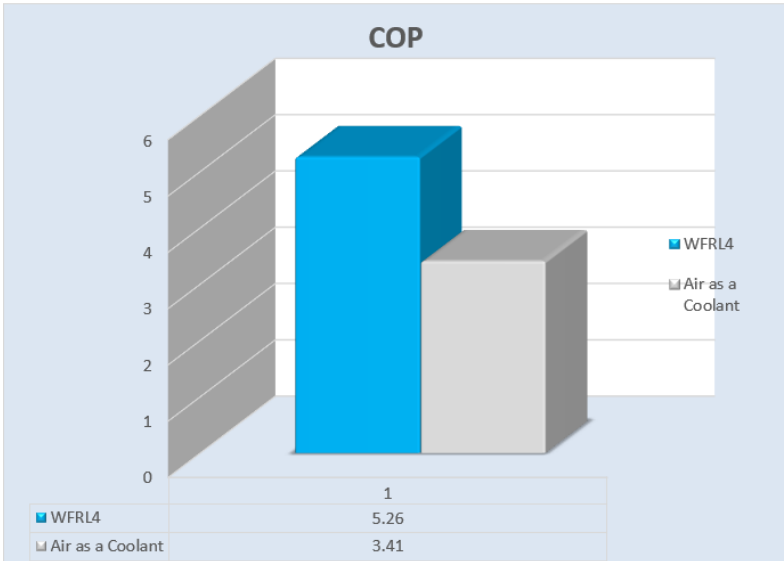

Figure 20. COP at the WFRL4 compared to using air as a refrigerant cooler

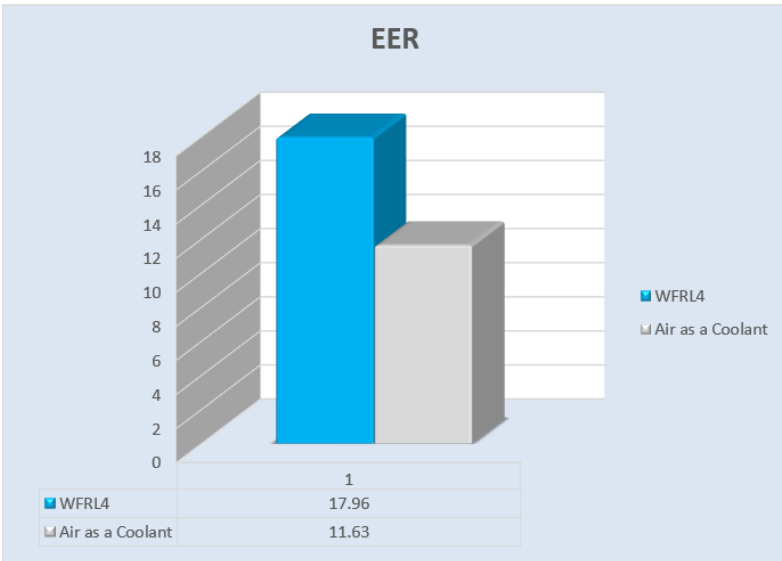

Figure 21. EER at the fourth water flow rate compared to using air as a refrigerant cooler

Figure 18 illustrates the total electrical current required for system operation, showing that the highest current draw, 20 amps, occurs at the first flow rate due to the compressor operating under unfavourable conditions, particularly high temperatures. In contrast, at the WFRL4, the compressor operated smoothly, resulting in a reduced current draw of only 9 amps. Figure 19 illustrates solar energy usage and surplus across flow rates. At the WFRL1, all energy was consumed by the cooling system, while the WFRL2 saved 10% for other devices but with inadequate cooling. The WFRL3 allowed 18% of energy for other devices, though cooling remained suboptimal. The WFRL4 demonstrated optimal efficiency, using 45% for cooling and 40% for other devices, leaving a 15% energy surplus. This confirms that the WFRL4 best supports optimal room conditions and exemplifies a "Zero Energy Building" model, fully relying on renewable energy with a surplus. After identifying the fourth flow rate as optimal, the system was compared to a commercial cooling system using air to cool the compressor outlet refrigerant. Using cold water resulted in a heat rejection of 10,438 Joules, compared to 6,820 Joules with air cooling, as shown in Figure 20. This enhances cooling system performance with water cooling, yielding a cooling COP of 5.26 versus 3.41 with air, improving cooling efficiency by 54%, as illustrated in Figure 21. Additionally, the EER increased significantly with water cooling, reaching 17.96 compared to 11.63 with air—also a 54% improvement. This is a crucial metric, especially as EER improvement has been emphasized in the Montreal Protocol, to which Iraq is a committed member for environmental protection.

5. CONCLUSIONS

The experimental study presented the development of an environmentally friendly hybrid cooling system that relies entirely on renewable energy sources. Four water flow rate levels were used, and the results proved that the cooling rate increases with an increase in flow rate. This is due to the larger heat exchange available for heat transfer from the refrigerant to the pre-cooled water by the ground's cool temperature. The study also demonstrated that the cooling rate at night is lower than during the day at all levels. This is due to thermal accumulation within the deep borehole, resulting from reverse heat transfer from the water supplied by the first tank to the water already present inside the borehole. The best water flow rate level was the fourth, with a flow rate of 18 liters per minute, for several reasons. The most important factor is that this level provided enough surface area to cool the refrigerant inside the WRHE, resulting in the highest WRHE effectiveness, which reached 79%. It also provided a high cooling rate, reducing the room temperature from above 40°C to 24°C. This modern system outperformed the air-cooled system in terms of performance, improving the COP by 54%. In terms of energy, the system provided a zero-energy building, with all devices powered by electricity generated from solar energy, and it even saved 15% of the supplied energy. Finally, this study offers a solution to reduce environmental pollution by achieving zero greenhouse gas emissions and minimizing energy consumption. We propose that researchers in this scientific field focus on advancing cooling systems based on solar and geothermal energy, as demonstrated in the model presented in this study. This development can be achieved by exploring various heat exchanger designs within the borehole, such as a W-shaped configuration or other geometric variations, to ensure sufficient heat exchange surface area for effective cooling. Additionally, the system can be improved by integrating phase change materials (PCMs) within the storage tanks, particularly in the Third tank, to maintain a continuous reduction in water temperature. Furthermore, further advancements can be made by investigating alternative working fluids instead of water to enhance the cooling efficiency of the refrigerant, potentially improving overall system performance and sustainability.

ACKNOWLEDGMENT

Gratitude is extended to Mr. Youssef Al-Hamdan for graciously offering a portion of his land in Karbala to conduct experimental experiments for the research.

REFERENCES

[1] Serale, G., Fabrizio, E., Perino, M. (2015). Design of a low-temperature solar heating system based on a slurry Phase Change Material (PCS). Energy and Buildings, 106: 44-58. http://doi.org/10.1016/j.enbuild.2015.06.063

[2] Wong, S.L., Wan, K.K., Li, D.H., Lam, J.C. (2010). Impact of climate change on residential building envelope cooling loads in subtropical climates. Energy and Buildings, 42(11): 2098-2103. https://doi.org/10.1016/j.enbuild.2010.06.021

[3] Congedo, P.M., Lorusso, C., De Giorgi, M.G., Marti, R., D'Agostino, D. (2016). Horizontal air-ground heat exchanger performance and humidity simulation by computational fluid dynamic analysis. Energies, 9(11): 930. https://doi.org/10.3390/en9110930

[4] Palomba, V., Bonanno, A., Brunaccini, G., Aloisio, D., Sergi, F., Dino, G.E., Frazzica, A. (2021). Hybrid cascade heat pump and thermal-electric energy storage system for residential buildings: Experimental testing and performance analysis. Energies, 14(9): 2580. https://doi.org/10.3390/en14092580

[5] Hussen, H.M., Hisham, A.H. (2010). Experimental model of ground source heat pump system. In Proceedings of the 7th Jordanian International Mechanical Engineering Conference (JIMEC'7), Amman, Jordan, pp. 27-29.

[6] Santos, A.F., de Souza, H.J., Cantao, M.P., Gaspar, P.D. (2016). Analysis of geothermal temperatures for heat pumps application in Paraná (Brasil). Open Engineering, 6(1): 485-491. https://doi.org/10.1515/eng-2016-0063

[7] Ghafoor, D.Z., Khdir, Y.K. (2020). Experimental investigation of earth tube heat exchanger (ETHE) for controlled ventilation in Erbil. In 2020 6th International Engineering Conference "Sustainable Technology and Development"(IEC), Erbil, Iraq, pp. 80-85. https://doi.org/10.1109/IEC49899.2020.9122908

[8] Omran, H.E., Hussain, T.A., Hachim, D.M. (2020). Study of two layers horizontal ground heat exchanger performance under a different operation mode. IOP Conference Series: Materials Science and Engineering 928(2): 022043. https://doi.org/10.1088/1757-899X/928/2/022043

[9] Yasukawa, K., Takashima, I., Uchida, Y., Tenma, N., Lorphensri, O. (2009). Geothermal heat pump

application for space cooling in Kamphaengphet, Thailand. Bulletin of the Geological Survey of Japan, 60(9-10): 491-501. http://doi.org/10.9795/bullgsj.60.491
[10] Hwang, Y., Lee, J.K., Jeong, Y.M., Koo, K.M., Lee, D.H., Kim, I.K., Kim, S.H. (2009). Cooling performance of a vertical ground-coupled heat pump system installed in a school building. Renewable Energy, 34(3): 578-582. https://doi.org/10.1016/j.renene.2008.05.042
[11] Naili, N., Attar, I., Hazami, M., Farhat, A. (2013). First in situ operation performance test of ground source heat pump in Tunisia. Energy Conversion and Management, 75: 292-301. https://doi.org/10.1016/j.enconman.2013.06.014
[12] Omer, A.M. (2020). Geothermal energy for refrigeration and air conditioning, sustainable development, and the environment. Journal of Drugs and Ecotoxicology, 3(2).
[13] Reda, F. (2017). Solar Assisted Ground Source Heat Pump Solutions: Effective Energy Flows Climate Management. Berlin/Heidelberg, Germany: Springer.
[14] Nouri, G., Noorollahi, Y., Yousefi, H. (2019). Solar assisted ground source heat pump systems–A review. Applied Thermal Engineering, 163: 114351. https://doi.org/10.1016/j.applthermaleng.2019.114351
[15] Roy, R., Bhowal, A.J., Mandal, B.K. (2020). Exergy and cost optimization of a two-stage refrigeration system using refrigerant R32 and R410A. Journal of Thermal Science and Engineering Applications, 12(3): 031024. https://doi.org/10.1115/1.4046253
[16] McQuiston, F.C., Parker, J.D., Spitler, J.D. (1994). Heating, Ventilating, and Air Analysis & Design. 4th Edition, John Willey & Sons, Inc.
[17] Janssen, J.E. (1989). Ventilation for acceptable indoor air quality. Ashrae Journal, 40-48.
[18] ASHRAE Standard (1992). Thermal environmental conditions for human occupancy. ANSI/ASHRAE, 55: 5.
[19] Olatunde, T.M., Okwandu, A.C., Akande, D.O. (2024). Reviewing the impact of energy-efficient appliances on household consumption. International Journal of Science and Technology Research Archive, 6(2): 1-11. https://doi.org/10.53771/ijstra.2024.6.2.0038
[20] Bergman, T.L. (2011). Fundamentals of Heat and Mass Transfer. John Wiley & Sons.
[21] Adam, M., Tokar, A. (2019). Energy efficiency in HVAC system using air cooling by direct evaporation. Acta Technica Corviniensis–Bulletin of Engineering, 12: 57-61.
[22] Uddin, K., Saha, B.B. (2022). An overview of environment-friendly refrigerants for domestic air conditioning applications. Energies, 15(21): 8082. https://doi.org/10.3390/en15218082
[23] Liu, G., Chen, H., Yuan, Y., Song, C. (2024). Indoor thermal environment and human health: A systematic review. Renewable and Sustainable Energy Reviews, 191: 114164. https://doi.org/10.1016/j.rser.2023.114164
[24] Ness, M.C.A.E. (2022). Indoor relative humidity: Relevance for health, comfort, and choice of ventilation system. In Proceedings of 3rd Valencia International Biennial of Research in Architecture, Changing Priorities, Valencia, pp. 218-228. http://doi.org/10.4995/VIBRArch2022.2022.15237

NOMENCLATURE

ΔTF (°C)	the temperature difference between the inside surface and the indoor temperature
12SS2	12: Indicates the number of input/output (I/O) points. SS: This stands for Slim Standard, a compact, basic PLC design. 2: Refers to the generation/version of the PLC.
A	area, m^2
Ad	surface area of a door, m^2
DOP-107V	DOP Stands for Delta Operator Panel 107: Refers to the model's screen size V: Indicates the version or series of the panel
I	electric current, ampere
P	Power, watt
Q	cooling load, joule
QL	total lighting heat load, joule
Qg/cond	the heat gain due to conduction through glass, joule
Qg/sol	solar heat gain through a glass, joule
Qinf/L	latent heat load due to air infiltration, joule
Qinf/S	sensible heat load due to air infiltration, joule
Qp/L	the latent heat load due to the presence of people, joule
Qp/S	the sensible heat load due to the presence of people, joule
Qrej	rejected heat, joule
Qvent/L	the latent heat gain, joule
Qvent/S	the sensible heat gain, joule
Ti	inside air temperature, °C
To	outside air temperature, °C
Tw	water temperature, °C
U	thermal transmittance, $W/m^2 \cdot K$
Ud	thermal transmittance of a door, $W/m^2 \cdot K$
Ug	U-value of the glass (thermal transmittance), $W/m^2 \cdot K$
V	voltage
Vinf	infiltration rate, m^3/h
Vvent	ventilation rate, m^3/h
Wi	inside air humidity ratio, kg/kg
Wo	outside air humidity ratio, kg/kg
qL/P	latent heat gain per person, w/m
qS/P	the sensible heat gain per person, w/m

Greek symbols

ϵexp	Experimental Effectiveness of Heat Exchanger

Subscripts

CLF	Cooling Load Factor
CLTD	Cooling Load Temperature Difference
CLTDc	Corrected Cooling Load Temperature Difference
COP	Coefficient of performance
CPU	Central Processing Unit
CWCS	Cooling Water Circulation System
DVP	Delta Variable Programmable
EER	Energy Efficiency Ratio
FB	Ballast factor
GSHP	Ground Source Heat Pump
H	Relative Humidity

HVAC	Heating, Ventilation, and Air Conditioning
MLC	Multi-Layer Composite
NL	The number of lighting fixtures in the space
No/p	The number of people present in the space
PCM	Phase change material
PLC	Programmable Logic Controller
PVC	Polyvinyl Chloride
RTD	Resistance Temperature Detectors
SAGSHP	Solar-Assisted Ground Source Heat Pump
SC	Shading Coefficient
SHGmax	Maximum Solar Heat Gain
WFTCU	Water Flow – Temperature Control Unit
WL	The wattage of each lighting fixture, indicating how much power each light consumes
WRHE	Water-Refrigerant Heat Exchanger
WWHE	Water-Water Heat Exchanger
WFRL	Water Flow Rate Level